Langmuir

ARTICLE

pubs.acs.org/Langmuir

Capillary Force between Wetted Nanometric Contacts and Its Application to Atomic Force Microscopy

Jérôme Crassous,[†] Matteo Ciccotti,[‡,⊥] and Elisabeth Charlaix[§,*]

[†]Institut de Physique de Rennes, UMR UR1-CNRS 6251, Université de Rennes 1, Campus de Beaulieu, F-35042 Rennes Cedex, France

[‡]Laboratoire des Colloides, Verres et Nanomatériaux, CNRS, Université Montpellier 2, Montpellier, France

[§]Laboratoire de Physique de la Matière Condensée et Nanostructures; CNRS, UMR 5586, Université de Lyon I, 69622 Villeurbanne, France

Supporting Information

ABSTRACT: We extend to the case of perfect wetting the exact calculation of Orr et al. (*J. Fluid. Mech.* **1975**, *67*, 723) for a pendular ring connecting two dry surfaces. We derive an approximate analytical expression for the capillary force between two highly curved surfaces covered by a wetting liquid film. The domain of validity of this expression is assessed and extended by a custom-made numerical simulation based on the full exact mathematical description. In the case of attractive liquid−solid van der Waals interactions, the capillary force increases monotonically with decreasing vapor pressure up to several times its saturation value. This accurate description of the capillary force makes it possible to estimate the adhesion force between wet nanoparticles; it can also be used to quantitatively interpret pull-off forces measured by atomic force microscopy.

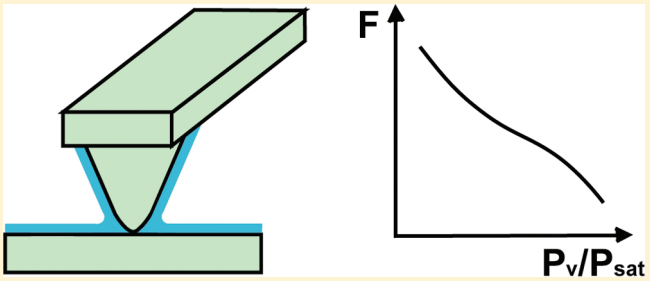

INTRODUCTION

As the size of systems goes down, surface effects become increasingly important. Capillary condensation, which results from the effect of surfaces on the phase diagram of a fluid, is a phenomenon that is ubiquitous at nanoscale and occurs in all confined geometries: divided media, cracks, or contacts between surfaces.[1,2] The very large capillary forces induced by highly curved menisci usually supersede other interaction forces and have a huge impact on the mechanical properties of solid contacts.[3] The tribological behavior and stiction phenomena in micro/nanoelectromechanical systems (MEMS/NEMS),[4] the cohesion and flow of powders and granular media,[5,6] the friction of sliding nanocontacts with aging effects, and enhanced stick−slip motion[7−10] are just a few examples of the huge impact of capillary forces at the nanoscale.

The great relevance of capillary forces between nanoscale objects to these topics has stimulated the utilization of contact AFM to provide a more quantitative measurement of the forces acting between the very sharp probe tip (with a typical radius of curvature of a few nanometers) and samples with variable compositions or textures.[11−16] However, most analyses have focused on the case of dry surfaces, i.e., the case of partial wetting for which the liquid−vapor meniscus connects directly onto the surfaces with a finite or zero contact angle.[17,18] This situation covers only a small part of the wetting situations favorable for capillary condensation. Liquid condensates between contacts are indeed prone to appear from an undersaturated vapor if the solid−liquid surface tension γ_{sl} is lower than that of the solid/vapor γ_{sv},[3] that is if the wetting parameter $S = \gamma_{sv} - \gamma_{sl} - \gamma_{lv}$ obeys the inequality $S > -\gamma_{lv}$ where γ_{lv} is the liquid−vapor surface tension. The partial wetting case corresponds to the domain $-\gamma_{lv} < S < 0$.[19] In the domain of perfect wetting $S \geq 0$, thin liquid films may also condense on the surfaces and connect smoothly onto the liquid bridge so that no liquid−solid−vapor contact lines exist anymore.[20]

The effect of wetting liquid films on the capillary force has been investigated quantitatively both theoretically and experimentally by the use of surface forces apparatus involving surfaces with a very large radius of curvature R. It is now well understood.[21−23] The wetting films cause the capillary force to decrease monotonically when the vapor pressure increases, from the value $F_{cap}/R = 4\pi\gamma_{sv}$ in a dry atmosphere down to $F_{cap}/R = 4\pi(\gamma_{sl} + \gamma_{lv})$ in a fully saturated atmosphere.[23] This behavior is usually not observed for AFM pull-off forces, which often report an increase of the capillary force with humidity.[12] This feature has been attributed to the roughness of the AFM tip, or samples.[14−16] However the experiments of Asay and Kim[24] clearly demonstrate the effect of condensed wetting films on the AFM pull-off forces. This effect was observed to increase with decreasing humidity up to several times the typical value $F_{cap}/R = 4\pi\gamma_{lv}$ obtained in saturating vapor. As quoted by the authors, even if the thickness of wetting films is usually in the nanometric range, these films

Received: September 23, 2010
Revised: January 16, 2011
Published: March 03, 2011

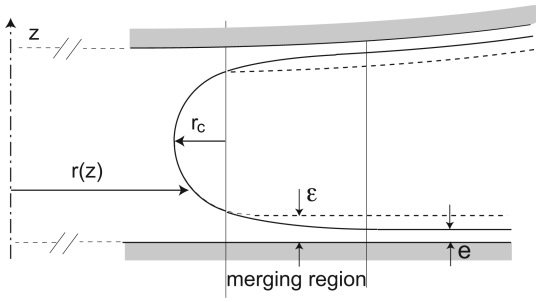

Figure 1. Merging of a meniscus on wetting films of nominal thickness e far from the bridge (not to scale). The dotted line represents a meniscus of circular shape connected tangentially to a virtual liquid film of thickness ε.

cannot be neglected when estimating the capillary force between nanoscale objects.[25,26]

In the present paper, we establish an analytical, yet approximate, expression for the capillary force between surfaces of nanometric curvature (two identical spheres or a sphere and a plane) in the presence of wetting liquid films, and we compare it with numerical solutions of the capillary and disjoining pressure equations. The analytical expression takes into account the noncircular shape of the liquid−vapor meniscus due to its axisymmetric curvature, as well as any type of disjoining pressure and wetting potential governing the liquid film. Our analytical expression, eq 9, is an expansion in powers of r_c/R and ε/R, where R is the sphere radius, r_c is the equilibrium curvature radius of the interface (Kelvin's radius), and ε is the apparent film thickness (defined by eq 4). The coefficients of this expansion have numerical values that are independent of the disjoining pressure and wetting interface potential. The range of validity of the analytical expression covers a wide range of vapor pressures, and is assessed by a comparison with numerical solutions of the equilibrium meniscus shape. The effect of surface roughness can be easily incorporated in this expression of the capillary force. We discuss the application of our expression in three situations: (i) the capillary force exerted by water condensed between nanometric glass spheres, using a van der Waals wetting potential; (ii) the effect of surface roughness on this capillary force; (iii) the comparison to AFM pull-off force measurements by Asay and Kim[24] under various alcohol vapor pressures.

■ ANALYTICAL THEORY

Our starting point is the case of the very large sphere radius $R \gg r_c$ in which the azimuthal curvature due to the axisymmetric shape of the liquid bridge can be neglected. The magnitude of the azimuthal radius of curvature is indeed of order $(2r_cR)^{1/2} \gg r_c$, if $R \gg r_c$ (see Figure 1). The shape of the meniscus connected to the liquid films covering the surfaces can then be solved in a 2D approximation. This has been done independently by Derjaguin[27] and Legait and de Gennes[28] in the context of the interface potential and disjoining pressure theory. The liquid film thermodynamics is described by the interface potential $W_{slv}(e)$ acting per unit area of the (flat) liquid/gas interface interacting with the solid surface. The pressure P_{liq} in the liquid film far from the bridge is given by the disjoining pressure:

$$\Pi_d(e) = -\frac{dW_{slv}}{de} = P_{ext} - P_{liq} \qquad (1)$$

with P_{ext} the pressure of the atmosphere. For nonretarded van der Waals forces the disjoining pressure is $\Pi_d(e) = -A_{slv}/6\pi e^3$ where A_{slv} is the solid/liquid/vapor Hamaker constant. For long-range electrostatic interactions, it is $\Pi_d(e) = (\pi\varepsilon_o/8e^2)(k_BT/q)^2$, where ε_o is the dielectric constant and q is the ionic charge; however the application of the Derjaguin equation in this specific case may be more questionable due to the larger impact of curvature on surface forces.[29] Short range structural interactions are usually described by an exponential-type disjoining pressure $\Pi_d(e)=K\exp(-e/\lambda)$, where K and λ are the amplitude and range of the interaction.[29]

At thermodynamic equilibrium, the liquid pressure in the film is the same as in the liquid bridge. The latter is determined by the capillary pressure drop γ_{lv}/r_c across the meniscus of curvature radius r_c. This assumes that the direct interaction of the meniscus with the solid wall is negligible in its central region, that is $\Pi_d(r_c) \ll \Pi_d(e) = \gamma_{lv}/r_c$. As the disjoining pressure is a rapidly decaying function of e this is usually satisfied for $e < r_c$. Therefore, we limit to the domain $e < 0.3r_c$ the validity of our analytical theory of the capillary force. The equilibrium thickness of the film covering the flat plane far from the bridge is then related to the meniscus curvature by

$$\Pi_d(e) = \frac{\gamma_{lv}}{r_c} \qquad (2)$$

If the liquid is volatile, the equilibrium of the liquid bridge curvature with its vapor phase is given by Kelvin's law:

$$\frac{\gamma_{lv}}{r_c} = \rho_L\Delta\mu = \rho_L k_B T \ln\frac{P_{sat}}{P_v} \qquad (3)$$

where $\Delta\mu$ is the vapor undersaturation, ρ_L the liquid molecular density, P_v/P_{sat} the relative humidity, k_B the Boltzmann constant, and T the temperature.

In the region where the meniscus merges onto the wetting films, its interaction with the solid wall is not negligible, and the pressure in the liquid is the sum of the disjoining pressure and of the local capillary pressure. The meniscus curvature is not constant and decays from r_c^{-1} to 0. This leads to a local thickening of the wetting film equal to:[27,28]

$$\varepsilon = e + \frac{W_{slv}(e)}{\Pi_d(e)} \qquad (4)$$

so that the overall geometry is equivalent to a meniscus of constant radius of curvature r_c merging with a zero contact angle onto a virtual film of thickness ε. This merging region and the associated thickening of the wetting film have been directly observed by an interferometric technique in the case of nonretarded van der Waals forces by Kolarov et al.[30] The capillary force in this 2D picture is then simply obtained by stating that when the virtual films come into contact, the capillary force has the standard value for $R \gg r_c$ with a zero contact angle:[3]

$$F_{cap}(D = 2\varepsilon) = 4(2)\pi\gamma_{lv}R$$

Here the number (2) between parentheses stands for the sphere−sphere (ss) case. As the variation of the capillary force with the distance is linear when $R \gg r_c$,[3] the maximum capillary force obtained at contact is

$$\frac{F_{sp(ss)}}{2\pi\gamma_{lv}R} = 2(1)\left[1 + \frac{\varepsilon}{r_c}\right] \qquad (5)$$

where sp (respectively ss) refers to the sphere-plane geometry (respectively sphere−sphere) and the number in parentheses stands for the (ss) case. This is the expression obtained by Christenson et al.[22] and Charlaix et al.[23]

dx.doi.org/10.1021/la103781y |Langmuir 2011, 27, 3468–3473

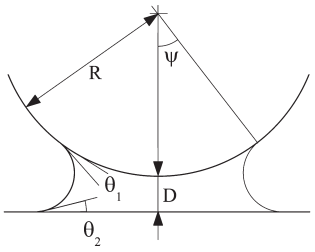

Figure 2. Pendular liquid bridge between a sphere and a plane.

Our basic assumption to address the case of a small sphere radius is that the physics of the merging region is not affected by the additional 3D curvature. The azimuthal curvature of an axisymmetric surface defined by its profile $r(z)$ around the Oz axis, equal to $1/r(1 + (dr/dz)^2)^{1/2}$, becomes indeed negligible in the merging region where dr/dz diverges. Therefore, as in the 2D case, the shape of the meniscus is equivalent to a meniscus of constant mean curvature $1/r_c$ merging with a zero contact angle on virtual solid surfaces obtained from the real ones by complementing them with a layer of constant thickness ε, as given by eq 4. But now the mean curvature $1/r_c$ includes the azimuthal curvature. The problem of an axisymmetric meniscus of constant mean curvature between a sphere and a plane has been solved by Orr et al.[31] We use their solution, taking a virtual sphere radius $R + \varepsilon$ to take into account the merging on the complemented sphere, and a distance $D - 2\varepsilon$ between the virtual surfaces. The solution by Orr's et al. is expressed in terms of the mean dimensionless meniscus curvature HR where $H = -1/2r_c$, the filling angle ψ defined at the level of the contact line on the sphere, and the contact angles θ_1 on the sphere and θ_2 on the plane (see Figure 2):

$$2HR = \Psi\left[\Theta - \frac{1}{k}[E(\phi_2,k) - E(\phi_1,k)] + \frac{1-k^2}{k}[F(\phi_2,k) - F(\phi_1,k)]\right] \quad (6)$$

with

$$\Psi = 1/(\delta + 1 - \cos\psi)$$
$$\Theta = -\cos(\theta_1 + \psi) - \cos\theta_2$$
$$\phi_1 = -(\theta_1 + \psi) + \pi/2$$
$$\phi_2 = \theta_2 - \pi/2$$
$$k = 1/(1 + c)^{1/2}$$
$$c = 4H^2R^2\sin^2\psi - 4HR\sin\psi\sin(\theta_1 + \psi)$$
$$H = -1/2r_c$$

δ=D/R is the reduced sphere-plane distance and E, F are the incomplete elliptic integrals of the first and second kinds. The sphere-plane geometry corresponds in our case to $\theta_1 = \theta_2 = 0$, whereas the sphere−sphere geometry is $\theta_1 = 0$ and $\theta_2 = \pi/2$. The capillary force is the sum of the tension force and of the capillary pressure force:[31]

$$F = 2\pi R\gamma_{lv}[\sin\psi\sin(\theta_1 + \psi) - HR\sin^2\psi] \quad (7)$$

The set of eqs 6 and 7 does not permit one to obtain an exact analytical solution for ψ as a function of r_c/R, and thus an analytical expression of the capillary force as a function of r_c/R and D/R. We propose here to approximate the capillary force by an expansion in powers of these parameters. The expansion is performed with the software Mathematica[32] and the details are provided in the Supporting Information. We address both the sphere−sphere and the sphere-plane case. We find:

$$\frac{F}{2\pi\gamma_{lv}R} = \alpha_o\left(1 - \frac{D}{2r_c}\right) + \alpha_1\left(1 + \frac{D}{4r_c}\right)\left(\frac{r_c}{R}\right)^{1/2} + \alpha_2\frac{r_c}{R} \quad (8)$$

where the α_i have numerical values given in Table 1. We obtain the maximum capillary force at contact between the surfaces, by replacing R with $R + \varepsilon$ and D with -2ε in 8:

$$\frac{F_{cap}}{2\pi\gamma_{lv}R} = \alpha_o\left(1 + \frac{\varepsilon}{r_c}\right) + \alpha_1\left(1 - \frac{\varepsilon}{2r_c}\right)\left(\frac{r_c}{R}\right)^{1/2} + \alpha_2\frac{r_c}{R} \quad (9)$$

The leading order of this expansion is nothing else than the capillary force for large sphere radius expressed in eq 5, and measured in Surface Force experiments.[22,23] The filling angle ψ is:

$$\psi = \beta_o\sqrt{\frac{r_c}{R}}\left(1 + \frac{\varepsilon}{2r_c}\right) - \frac{\pi}{8}\frac{r_c}{R} \quad (10)$$

For the sake of simplicity and without restriction we have assumed in the calculation that both surfaces have similar wetting properties. In the general case of asymmetric wetting properties, the overthickness ε should be replaced by the mean value $(\varepsilon_s + \varepsilon_p)/2$ where the $\varepsilon_{s,p}$ obey eq 4 applied on each surface with its own disjoining pressure and wetting potential.

Finally, we should mention that expressions 9 and 10 are only valid if thermodynamically stable wetting films can form on the surfaces, which requires the grand potential of the wet surface $\gamma_{sl} + \gamma_{lv} + W_{slv}(e) + e\Pi_d(e)$ to be lower than the one of the dry surface, γ_{sv}.[20,33] Taking into account eqs 2 and 4 this may be written as

$$\gamma_{sl} + \gamma_{lv}\left(1 + \frac{\varepsilon}{r_c}\right) \le \gamma_{sv} \quad (11)$$

If eq 11 is not verified then the surfaces remain dry.[20,33] Multiplying eq 11 by $4\pi R$ ($2\pi R$ in the ss case), we get on the right-hand side the adhesion force between the ideally smooth dry solids. The left-hand side is the total adhesion force for $R \gg r_c$, consisting of the direct solid adhesion force through the liquid, and of the capillary force given in eq 5. However, expression 9 gives a capillary force that is always smaller than in the $R \gg r_c$ case. Therefore, for ideally smooth solids the capillary force can never be larger than the adhesion force between dry solids, which should be recovered at very low vapor pressure.

NUMERICAL COMPUTATION OF THE CAPILLARY FORCE

In order to estimate the accuracy of the approximate expression established above, we develop in this section a numerical calculation of the capillary force based on the exact shape of the liquid−vapor interface that smoothly connects the liquid bridge to the wetting films. For simplicity reasons, we restrict this numerical section to the interaction between two spheres. The starting point of our derivation is the grand potential of the liquid that connects two wet spheres as shown in Figure 3. The

Table 1. Numerical Values of the Coefficients in the Analytical Expressions Eqs 9 and 10 of the Capillary Force and Filling Angle

	α_o	α_1	α_2	β_o
sphere−plane	2	$-(\pi)/(4) = -0.7854$	$-(\pi^2)/(64) = -0.1542$	2
sphere−sphere	1	$-(\pi)/(4(2)^{1/2}) = -0.555$	$(1)/(2) - (\pi^2)/(64) = 0.346$	$(2)^{1/2}$

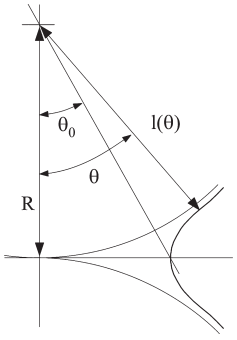

Figure 3. Liquid bridge connecting two spheres.

potential may be written as[34]

$$\Omega = 4\pi\gamma_{lv}\int_{\theta_0}^{\infty} l[l^2 + l_\theta{}^2]^{1/2}\sin\theta\,\mathrm{d}\theta + \Delta\mu\left[4\pi\int_{\theta_0}^{\infty}\frac{l^3\sin\theta}{3}\mathrm{d}\theta + \frac{2\pi R^3\tan^2\theta_0}{3} - \frac{8\pi R^3}{3}\right] + 4\pi\int_{\theta_0}^{\infty} W_{slv}(l-R)R^2\sin\theta\,\mathrm{d}\theta \quad (12)$$

where l is the distance between the interface and the center of the sphere, and l_θ is the derivative of l with respect to θ. In the right-hand side of 12, the first term is the solid−liquid interface energy, the second one is the energy associated with the volume of the condensed liquid, and the last one takes into account liquid−solid interactions. The Euler−Lagrange minimization $\partial\Omega/\partial l = \mathrm{d}(\partial\Omega/\partial l_\theta)/\mathrm{d}\theta$ of 12 then yields:

$$l_{\theta\theta}l - 3l_\theta{}^2 - 2l^2 + \mathrm{cotan}\,\theta\,\frac{(l^2 + l_\theta^2)l_\theta}{l} + (l^2 + l_\theta{}^2)^{3/2}\left[\frac{\Delta\mu}{\gamma_{lv}} + \frac{R^2}{l^2\gamma_{lv}}\frac{\mathrm{d}W_{slv}(l-R)}{\mathrm{d}e}\right] = 0 \quad (13)$$

where $l_{\theta\theta}$ is the second derivative of l with respect to θ. The boundary conditions of eq 13 are $l_\theta(\pi) = 0$, $l(\theta_0)\cos\theta_0 = R$ and $l_\theta(\theta_0) = -R\sin\theta_o$, with θ_0 a parameter to be determined. We solved 13 using an adaptive step size Runge−Kunta algorithm.[35] Starting from an initial value θ_0, 13 is integrated for increasing values of θ. The θ_0 value is adjusted iteratively to ensure that l_θ vanishes when $l = R + e$. Finally, the force is computed as $F_{ss}^{(wet)}/2\pi R\gamma_{lv} = R\tan^2\theta_0/2r_c + R\tan\theta_0$.

Figure 4 is a plot of the adhesion force as a function of the radius of curvature r_c/R for different values of e/r_c. The calculations are done for non retarded van der Waals forces, i.e., $\mathrm{d}W_{slv}/\mathrm{d}e \sim e^{-3}$. We clearly see that the adhesion force varies with both r_c/R and e/r_c. We can compare the numerical results with the results of the analytical expansion 9. For this, we fit the

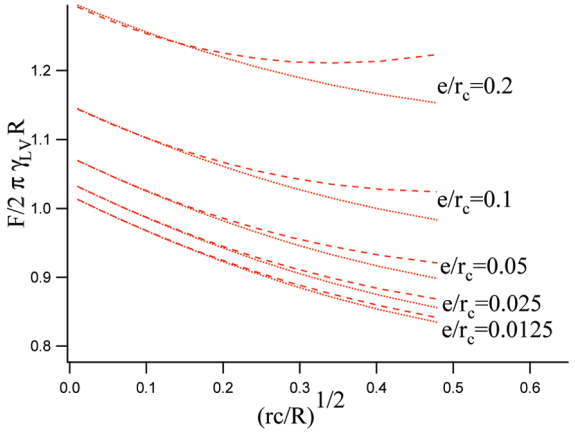

Figure 4. Dashed lines: normalized adhesion force evaluated numerically as a function of the square root of the reduced radius of curvature r_c/R. The dotted lines are the analytical expansion (eq 9) for the force. Different curves correspond to different values of e/r_c.

Table 2. Maximum Error ΔF Made on the Capillary Force by Using the Analytical Expansion 9 with Coefficients from the Last Line of Table *1* Instead of the Numerical Computation[a]

	$r_c/R < 0.01$	$r_c/R < 0.03$	$r_c/R < 0.10$	$r_c/R < 0.3$
$e/r_c < 0.01$	1.9×10^{-4}	6.3×10^{-4}	2.3×10^{-3}	4.6×10^{-3}
$e/r_c < 0.03$	4.3×10^{-4}	1.4×10^{-3}	6.0×10^{-3}	1.8×10^{-2}
$e/r_c < 0.10$	8.5×10^{-4}	2.8×10^{-3}	1.3×10^{-2}	3.6×10^{-2}
$e/r_c < 0.30$	9.5×10^{-3}	9.5×10^{-3}	3.8×10^{-2}	1.6×10^{-1}

[a] Errors are in unit of $2\pi R\gamma_{lv}$. Errors are always lower than the maximal error displayed here when r_c/R is lower than the column value and e/r_c is lower than the line value. The calculation is made for a power law-type interface potential in the form $W_{slv}(e) \sim e^{-n}$ with n = 3, 4, and 5.

function $F_{ss}^{(wet)}/2\pi R\gamma_{lv} - 1 = A + Br_c^{1/2} + Cr_c + Dr_c^{3/2}$, for $10^{-6} < r_c/R < 10^{-2}$ and for every fixed value of e/r_c. The coefficients A, B, C, and D depend on e/r_c. We fit these dependences on e/r_c as $A = A_1 \times (e/r_c)$, $B = B_0 + B_1 \times (e/r_c)$ and as $C = C_0 + C_1 \times (e/r_c)$ for $10^{-4} < e/r_c < 10^{-3}$ The values of the coefficients are A_1 = 1.500 (expected value from numerical expansion 9: 3/2), $B_0 = -0.555$ (expected $-\pi/4(2)^{1/2} \simeq -0.555$), B_1 = 0.407 (expected $3\pi/16(2)^{1/2} \simeq 0.416$) and C_0 = 0.349 (expected $^1/_2 - \pi^2/64 \simeq 0.346$). Those agreements validate both the numerical algorithm and the analytical expansion 9.

Finally we evaluate the overall error on the capillary force made by using the analytical expansion 9. We compute the force F_{num} using the numerical solution and the force F_{ana} using the analytical expansion. The absolute difference $\Delta F = |F_{num} - F_{ana}|/2\pi\gamma_{lv}R$ usually increases with r_c/R and e/r_c. Table 2 shows the maximum force error ΔF for all values of r_c/R and of e/r_c lower than the values reported in the heads of the columns or lines. We see that the error is always lower than a few percents, except when r_c/R and e/r_c are together of order ~0.3.

dx.doi.org/10.1021/la103781y |*Langmuir* 2011, 27, 3468–3473

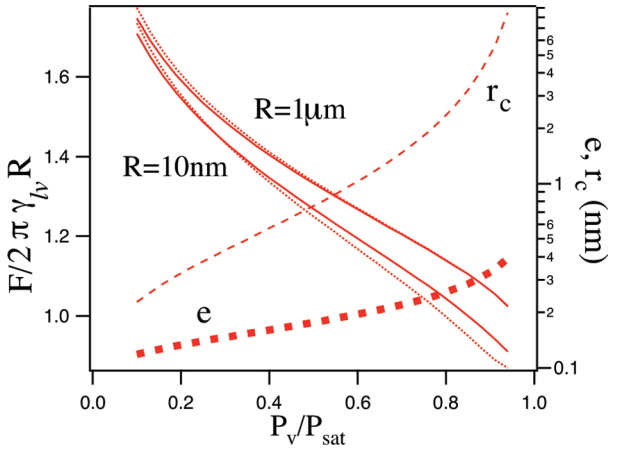

Figure 5. Normalized adhesion force between two silica spheres of radius R as a function of the relative humidity P_v/P_{sat}. The nominal wetting film thickness and the Kelvin radius are plotted as well. The wetting potential corresponds to van der Waals interactions with a Hamaker constant $A_{slv} = 0.85 \times 10^{-20}$ J. Plain lines are the numerical calculations of the capillary force obtained for $R = 10$ nm and $R = 1\ \mu$ m; dotted lines are the analytical expansions 9.

DISCUSSION

We illustrate our results by computing the capillary pull-off force exerted on a sphere of radius 10 nm modeling a sharp silicon AFM tip covered by its native oxide, in contact with a silica surface in a water vapor atmosphere. As wetting potential, we use nonretarded van der Waals interactions with a Hamaker constant $A_{slv} = 0.85 \times 10^{-20}$ J.[3] We do not illustrate here the effect of structural interactions, whose amplitude and range depend on the surface density of silanol groups.[36]

As shown in Figure 5, even for this sharp tip the analytical expansion provides a very good approximation of the capillary force, within 5%, up to a relative humidity of about 80%. The Kelvin radius of the water meniscus and the thickness of the wetting films are also plotted on the same graph. The same calculation is performed for a colloidal probe made of a silica sphere of radius 1 μm glued on the cantilever. For this radius, the analytical expression is almost not distinguishable from the exact capillary force.

Figure 5 shows that, in the case of perfect wetting, the capillary force decreases with increasing humidity. This is expected since in this case the surface tension of the dry solid is higher than the sum of the liquid−solid and liquid−vapor surface tension, which determine respectively the adhesion work of the surfaces in the liquid phase and the capillary force. The decrease of the pull-off force with increasing humidity has been observed in SFA experiments.[23,37] It is usually not found on the full range of relative humidity in AFM pull-off forces, where to the contrary the pull-off force increases with relative humidity at low humidity.[12] The increase of the capillary force with humidity is usually attributed to the roughness of the AFM tip or sample, preventing the surfaces to come to close contact.[14−16] In a model proposed by Rabinovitch et al.,[15] the effect of roughness on the capillary force is simply taken into account by introducing an offset distance h_o which is the average distance between the surfaces when the highest asperities are in contact. The adhesion force is then assumed equal to the dry adhesion force if the meniscus height is lower than h_o, otherwise it is kept equal to the capillary force between smooth surfaces at a distance $D = h_o$. This

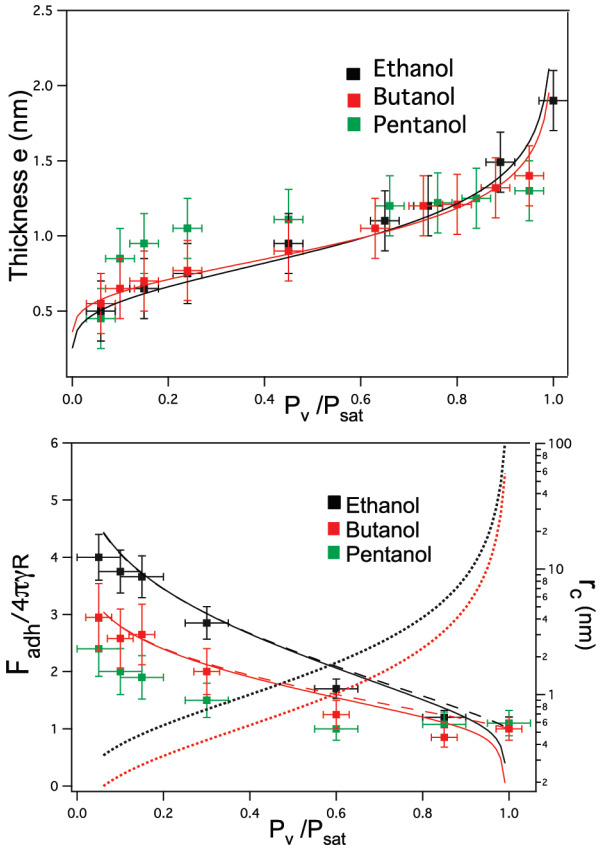

Figure 6. Top: adsorption isotherm of ethanol, 1-butanol and 1-pentanol on silicon wafer, measured by Asay and Kim.[24] The continuous line is the best fit of the isotherm with a disjoining pressure $\Pi_d(e) = K \exp(-e/\lambda)$. $K = 7 \times 10^8$ N/m^2 and $\lambda = 2.8$ Å for ethanol and $K = 8.3 \times 10^8$ N/m^2, $\lambda = 2.4$ Å for butanol. Bottom: Normalized AFM pull-off forces between a silicon cantilever of radius $R = 15$ nm and a silicon wafer in ethanol, 1-butanol, and 1-pentanol atmospheres.[24] The data were replotted. The continuous lines are the analytical expression 9 of the capillary force obtained without adjustable parameter from the best fit of the adsorption isotherms. Dashed lines correspond to the large sphere approximation 5. The dotted lines are the calculated Kelvin radii.

model is easily transcribed in our analytical expression, by replacing D with $h_o - 2\varepsilon$ instead of -2ε in eq 8.

Finally, we compare in figure Figure 6 our analytical expression to the experimental measurements of Asay et al.[24] of the AFM pull-off forces between a silicon cantilever and a silicon wafer in alcohol atmospheres. They measured the adsorption isotherms as well on the same samples. We fit these isotherms with a disjoining pressure of the form $\Pi_d(e) = K \exp(-e/\lambda)$, corresponding to short-range structural interactions.[29] The analytical capillary forces corresponding to these disjunction pressures, for the tip radius $R = 15$ nm used in the experiments, are plotted in figure Figure 6 without adjustable parameters. The physical constants of the liquids taken from ref 24 are $\gamma_{lv} = 21.8$ mN/m and $\rho_L = 1.7 \times 10^4$ mol/m^3 for ethanol, and $\gamma_{lv} = 24.6$ mN/m and $\rho_L = 1.1 \times 10^4$ mol/m^3 for butanol. The theoretical capillary force is in very good agreement with the measured pull-off forces, except at vapor pressure above 90% relative humidity where the Kelvin's radius becomes as large as the tip radius. It should be mentioned that the contribution of direct van der Waals interaction of the solids through the liquid, estimated from a typical Hamaker constant of $10^{-20}J$ and a cutoff distance of

dx.doi.org/10.1021/la103781y |*Langmuir* 2011, 27, 3468–3473

0.2 nm, is negligible compared to the capillary force. The pentanol is not plotted since its isotherm cannot be fitted with a simple power law or exponential disjoining pressure.

CONCLUSION

We have established a simple analytical expression of the capillary force between highly curved surfaces in the presence of wetting films, which we believe is of interest for predicting quantitatively the adhesion force between nano-objects. This expression can be used to estimate the adhesion between nanoparticles of high surface energy, whose surface is often covered by a contaminating liquid layer. We have also shown that it provides a simple method for the quantitative interpretation of AFM pull-off forces in a controlled vapor atmosphere.

ASSOCIATED CONTENT

Supporting Information. Starting from Orr's eqs 6 and 7 in the text, the capillary force and the filling angle are expanded in powers of $(r_c/R)^{1/2}$ and D/R for the sphere−sphere and the sphere-plane case. This material is available free of charge via the Internet at http://pubs.acs.org.

AUTHOR INFORMATION

Corresponding Author

*E-mail: elisabeth.charlaix@univ-lyonl.fr.

Present Address

[⊥]Laboratoire PPMD-SIMM, UMR CNRS 7615, ESPCI, 10 rue Vauquelin, 75005, Paris, France.

ACKNOWLEDGMENT

This work was supported by the ANR Grant "Corcosil" No. ANR-07-BLAN-0261-02

REFERENCES

(1) Bowden, F. P.; Tabor, D. *Friction and lubrication of solids*; Clarendon Press Oxford: Oxford, U.K., 1950.
(2) Charlaix, E.; Ciccotti, M. In *Handbook of Nanophysics: Principles and Methods*; Sattler, K., Ed.; CRC Press: Boca Raton, FL, 2010; Chapter 12, Capillary condensation in confined media.
(3) Israelachvili, J. *Molecular and Surface Forces*; Academic Press: New York, 1985.
(4) *Handbook of Nanotechnology*; Bhushan, B., Ed.; Springer: New York, 2007.
(5) Zimon, A. *Adhesion of dust and powder*; Plenum Press: New York, 1969.
(6) Hornbaker, D. R.; Albert, I.; Barabasi, A. L.; Shiffer, P. *Nature* **1997**, *387*, 765–766.
(7) Crassous, J.; Bocquet, L.; Ciliberto, S.; Laroche, C. *Europhys. Lett.* **1999**, *47*, 562–567.
(8) Riedo, E.; Levy, F.; Brune, H. *Phys. Rev. Lett.* **2002**, *88*, 185505.
(9) Restagno, F.; Ursini, C.; Gayvallet, H.; Charlaix, E. *Phys. Rev. E* **2002**, *66*, 021304.
(10) Feiler, A.; Stiernstedt, J.; Theander, K.; Jenkins, P.; Rutland, M. *Langmuir* **2007**, *23*, 517–522.
(11) Eastman, T.; Zhu, D.-M. *Langmuir* **1996**, *12*, 2859–2862.
(12) Xiao, X.; Qian, L. *Langmuir* **2000**, *16*, 8153–8158.
(13) Malotky, D. L.; Chaudhury, M. K. *Langmuir* **2001**, *17*, 7823–7829.
(14) He, M.; Blum, A.; Aston, D.; Buenviaje, C.; Overney, R. *J. Chem. Phys.* **2001**, *114*, 1355.
(15) Rabinovitch, Y.; Adler, J.; Ezayanor, M.; Ata, A.; Singh, R.; Moudgil, B. *Adv. Colloid Interface Sci.* **2002**, *96*, 213–230.
(16) Farshchi-Tabrizi, M.; Kappl, M.; Cheng, Y.; Gutmann, J.; Butt, H.-J. *Langmuir* **2006**, *22*, 2171–2184.
(17) de Lazzer, A.; Dreyer, M.; Rath, H. *Langmuir* **1999**, *15*, 4551–4559.
(18) Pakarinen, O. H.; Foster, A. S.; Paajanen, M.; Kalinainen, T.; Katainen, J.; Makkonen, I.; Lahtinen, J.; Nieminen, R. M. *Modelling Simul. Mater. Sci. Eng.* **2005**, *13*, 1175–1186.
(19) de Gennes, P.; Brochard, F.; Quéré, D. *Capillarity and Wetting Phenomena: Drops, Bubbles, Pearls, Waves*; Springer: New York, 2003.
(20) Joanny, J.; Léger, L. *Rep. Prog. Phys.* **1992**, *55*, 431.
(21) Crassous, J.; Charlaix, E.; Loubet, J. *Europhys. Lett.* **1994**, *28*, 37–42.
(22) Christenson, H. *Phys. Rev. Lett.* **1994**, *73*, 1821–1824.
(23) Charlaix, E.; Crassous, J. *J. Chem. Phys.* **2005**, *122*, 184701.
(24) Asay, D. B.; Kim, S. H. *Langmuir* **2007**, *23*, 12174–12178.
(25) Asay, D.; de Boer, M.; Kim, S. *J. Adhesion Sci. Technol* **2010**, *24*, 2363–2382.
(26) Hsiao, E.; Marino, M.; Kim, S. *J. Colloid Interface Sci.* **2010**, *352*, 549–557.
(27) Derjaguin, B.; Churaev, N. *J. Colloid Interface Sci.* **1976**, *54*, 157.
(28) Legait, B.; de Gennes, P. *J. Phys., Lett.* **1984**, *45*, L–647.
(29) Churaev, N. V. *Adv. Colloid Interface Sci.* **2003**, *103*, 197–218.
(30) Kolarov, T.; Zorin, Z.; Platikanov, D. *Colloids Surf.* **1990**, *51*, 37–47.
(31) Orr, F.; Scriven, L.; Rivas, A. *J. Fluid Mech.* **1975**, *67*, 723–742.
(32) Wolfram Research, I. *Mathematica ed., Version 5.0*, Champaign, IL, 2003.
(33) de Gennes, P. *Rev. Mod. Phys.* **1985**, *57*, 827.
(34) Dobbs, H.; Darbellay, G.; Yeomans, J. *Europhys. Lett.* **1992**, *18*, 439–444.
(35) Press, W.; Flannery, B.; Teukolsky, S.; Vetterling, W. *Numerical Recipes: the Art of Scientific Computing*; Cambridge University Press: Cambridge, U.K., 1986.
(36) Schlangen, L.; Koopal, L.; Cohen Stuart, M.; Lyklema, J. *Langmuir* **1995**, *11*, 1701–1710.
(37) Matsuoka, H.; Fukui, S. *Langmuir* **2002**, *18*, 6796–6801.